

## Article

# A Preliminary Study on the Mechanisms of Growth and Physiological Changes in Response to Different Temperatures in *Neopyropia yezoensis* (Rhodophyta)

Jiao Yin <sup>1</sup>, Aiming Lu <sup>1</sup> , Tuanjie Che <sup>2</sup>, Lihong He <sup>1,\*</sup> and Songdong Shen <sup>1,\*</sup>

<sup>1</sup> Department of Cell Biology, School of Biology and Basic Medical Sciences, Soochow University, No. 199 Renai Road, Suzhou 215123, China; 20194221017@stu.suda.edu.cn (J.Y.); 20204250021@stu.suda.edu.cn (A.L.)

<sup>2</sup> Key Laboratory of Functional Genomic and Molecular Diagnosis of Gansu Province, Lanzhou 730030, China; chetj@126.com

\* Correspondence: helh@suda.edu.cn (L.H.); shensongdong@suda.edu.cn (S.S.)

**Abstract:** As an economically valuable red seaweed, *Neopyropia yezoensis* (Rhodophyta) is cultivated in intertidal areas, and its growth and development are greatly influenced by environmental factors such as temperature. Although much effort has been devoted to delineating the influence, the underlying cellular and molecular mechanisms remain elusive. In this study, the gametophyte blades and protoplasts were cultured at different temperatures (13 °C, 17 °C, 21 °C, 25 °C). Only blades cultured at 13 °C maintained a normal growth state (the relative growth rate of thalli was positive, and the content of phycobiliprotein and pigments changed little); the survival and division rates of protoplasts were high at 13 °C, but greatly decreased with the increase in temperature, suggesting that 13 °C is suitable for the growth of *N. yezoensis*. In our efforts to delineate the underlying mechanism, a partial coding sequence (CDS) of Cyclin B and the complete CDS of cyclin-dependent-kinase B (CDKB) in *N. yezoensis* were cloned. Since Cyclin B controls G2/M phase transition by activating CDK and regulates the progression of cell division, we then analyzed how Cyclin B expression in the gametophyte blades might change with temperatures by qPCR and Western blotting. The results showed that the expression of Cyclin B first increased and then decreased after transfer from 13 °C to higher temperatures, and the downregulation of Cyclin B was more obvious with the increase in temperature. The phosphorylation of extracellular signal-regulated kinase (ERK) decreased with the increase in temperature, suggesting inactivation of ERK at higher temperatures; inhibition of ERK by FR180204 significantly decreased the survival and division rates of protoplasts cultured at 13 °C. These results suggest that downregulation of Cyclin B and inactivation of ERK might be involved in negatively regulating the survival and division of protoplasts and the growth of gametophyte blades of *N. yezoensis* at high temperatures.

**Keywords:** *Neopyropia yezoensis*; water temperature; growth; cyclin; extracellular signal-regulated kinase



**Citation:** Yin, J.; Lu, A.; Che, T.; He, L.; Shen, S. A Preliminary Study on the Mechanisms of Growth and Physiological Changes in Response to Different Temperatures in *Neopyropia yezoensis* (Rhodophyta). *Water* **2022**, *14*, 2175. <https://doi.org/10.3390/w14142175>

Academic Editor: José Luis Sánchez-Lizaso

Received: 9 May 2022

Accepted: 5 July 2022

Published: 9 July 2022

**Publisher's Note:** MDPI stays neutral with regard to jurisdictional claims in published maps and institutional affiliations.



**Copyright:** © 2022 by the authors. Licensee MDPI, Basel, Switzerland. This article is an open access article distributed under the terms and conditions of the Creative Commons Attribution (CC BY) license (<https://creativecommons.org/licenses/by/4.0/>).

## 1. Introduction

*Neopyropia* (Rhodophyta, Bangiaceae) is a genus of eurythermic macroalgae. Different species have different adaptabilities to environmental factors such as light and temperature; therefore, they are widely distributed in shallow intertidal zones of cold and subtropical regions [1]. *Neopyropia yezoensis* is a type of cultivated red seaweed that has immense economic value, which has been used as processed food or as a source of substances that promote health [2]. In addition, agar obtained from discolored *N. yezoensis* is successfully used in bacterial plate culture and DNA electrophoresis without agarose purification [3]. The annual production of *N. yezoensis* is about 1.8 million tons which estimated value about USD 1.5 billion [4]. The demand of *N. yezoensis* is increasing each year, leading to an increase in its cultivation scale [5]. *N. yezoensis* has diploid and haploid stages in its life cycle [6]; the haploid gametophyte blades (thalli) are the edible laver blades planted on the aquaculture

raft whose growth is affected by various ecological factors, such as temperature, salinity, and pH values [7,8]. Particularly, in recent years, rising seawater temperatures due to global warming [9] have put pressure on the cultivation of *Neopyropia* [10,11]. The differences in color and yield of *N. yezoensis* harvested at different periods are mainly impacted by temperature. Degradation and loss of photosynthetic pigments and phycobiliprotein will lead to the discoloration of the edible gametophytes and reduction in the quality of *N. yezoensis* product, negatively affecting the seaweed cultivation industry [12]. Therefore, the breeding of strains with high yield and strong tolerance has become an important topic in *N. yezoensis* cultivation [13]. Currently, many studies have been conducted worldwide to develop high-temperature-resistant (HTR) strains of *N. yezoensis* by ray mutagenesis and intraspecific hybridization on gametophytic blades of *N. yezoensis* [14–16]. However, these studies remained at the individual level, and the underlying molecular mechanisms have not been understood till date.

The net photosynthetic rate and pigment content can be used to characterize the growth of algae [17] and determine the quality of algal production and application [12,18]. The major photosynthetic pigments in gametophyte blades are as follows: chlorophyll (Chl), carotenoids, phycoerythrin (PE), phycocyanin (PC), and allophycocyanin (APC) [19,20]. Chl and carotenoids, as auxiliary pigments of photosynthesis, can effectively expand the range of light absorbed by plants and are necessary for energy production; they can also be used as a secondary antioxidant to prevent oxidation in response to oxidative stress by combining free oxygen or free radicals [21]. The quality of algae products is evaluated on the apparent blackness, which mainly arises from the photosynthetic pigments. For red algae, the distinctive color is due to phycobiliprotein [12,18,20]. The determination of photosynthetic parameters such as Chl fluorescence, photosynthetic pigment content, and photosynthetic oxygen evolution rate can be used to indicate improvement of stress tolerance and breeding efficiency of high-yield strains [19]. Temperature affects the contents of Chl *a* and phycobilins (PB) in *Geitlerinema amphibium* and *Pyropia tenera* [22,23]. When cultured at 0 °C, 5 °C, and 10 °C, the growth and development of *N. yezoensis* thalli were slow, resulting in decreased phycoerythrin contents as well as discolored thalli [24]. For *Chlamydomonas reinhardtii*, the photosynthetic rate is affected by temperature; the growth rate increases and the cell cycle duration shortens with an increase in temperature until the optimum temperature is attained, then the growth rate declines and cell cycle duration is prolonged [25].

Cells increase in number by cell division, producing smaller daughter cells; then, daughter cells grow by accumulating mass and increasing in size, leading to continuous growth of individual organisms. Coordinate regulation of cell growth and division rates determines cell size and individual growth [26,27]. To explore the molecular mechanisms underlying the growth and physiological changes of *N. yezoensis* in response to different temperatures, we focused on discovering molecules that regulate the mitotic phase.

The cell cycle progression of eukaryotes, including green algae, is primarily controlled by evolutionarily highly conserved serine/threonine kinases, termed cyclin-dependent-kinase (CDK)/cyclin complexes [28–30]. The cell cycle dependence on growth is associated with the attainment of cell cycle commitment points (CP) which are functionally equivalent to START in yeasts and restriction points in mammalian cells. Increasing temperature within normal physiological ranges results in increased growth and faster CP attainment. The CDK activity promotes the attainment of CP and mitosis. There are two related CDKs that regulate the progression of plant cell cycle, namely, CDKA and plant-specific CDKB [31,32]. CDKB transcription is activated in S/M cells [33]. The expression of Cyclin B occurs in the late G1 phase and accumulates gradually; it reaches the maximum value in the late G2 phase and maintains until metaphase, and then degrades rapidly [34].

Both biotic and abiotic stresses can induce a series of biological reactions by activating the mitogen-activated protein kinase (MAPK) signaling pathway, regulating cell functions related to various physiological, developmental, and plant hormone responses, thus affecting plant cell division and differentiation [35–37]. Many studies have shown the correlation

between extracellular regulated protein kinase (ERK), a member of MAPKs signal pathway, and cell division processes of many species. In synchronized *Chlamydomonas reinhardtii* cultures, the expression peaks of ERK-type MAPK genes appeared around S/M phase, in a manner similar to the main peak of CDKB, implying their functional involvement in S/M-phase entry [38]. p42/p44<sup>MAPK</sup> (ERKs) regulate the expression of cyclin and the activity of associated CDK activities that drives specific cell cycle responses to extracellular stimuli to participate in cell proliferation and differentiation [39]. Exposure of *Dunaliella viridiscell* to PD98059, a specific inhibitor of the ERK signaling pathway, caused a complete dephosphorylation of ERK and a total arrest of cell proliferation, indicating that activation of the ERK signaling pathway is required for cell proliferation [40].

As previously reported, temperature affects the growth and physiological metabolism of *N. yezoensis*; the optimal growth of the gametophyte thalli occurred at 10–15 °C [41], and was inhibited when cultured at 20 °C for 3 weeks [16]. To obtain a heat-resistant and high-yield strain of *N. yezoensis*, 23 °C and 24 °C were selected as the high temperature stress for screening [42,43]. In this study, we explored the cellular and molecular changes of *N. yezoensis* in response to high temperature stress at 17 °C, 21 °C, and 25 °C, respectively, and 13 °C was used as the normal control, laying a foundation for further revealing its cellular and molecular mechanism in response to adverse environmental conditions.

## 2. Materials and Methods

### 2.1. Algae and Culture Conditions

The fresh thalli of *N. yezoensis* (length: 3–4 cm) were collected from cultivation rafts, which were obtained from Rudong coasts, Jiangsu Province, China. The thalli were transported to the laboratory in an incubator containing ice packs. Thereafter, the thalli were cleaned thrice with artificially sterilized seawater. Then, the thalli were kept dry in the shade and stored at –80 °C for later use. Before performing the experiment, they were removed from the refrigerator and placed in artificially sterilized seawater in the illumination incubator for resuscitation for at least three days. The temperature was fixed at 13 °C, and the light intensity was fixed at 80  $\mu\text{mol photons m}^{-2} \text{s}^{-1}$  with a light period of 10 L:14 D. Each liter of sterilized seawater contains 1  $\mu\text{L}$  of Provasoli's enriched seawater (PES) medium. The seawater was changed every five days. After resuscitation, the thalli were cultured in sterilized seawater in illumination incubators at 13 °C, 17 °C, 21 °C, and 25 °C, respectively.

### 2.2. Measurement of Growth Rate

The fresh weight of the gametophyte blades was measured every 5 days to calculate the relative growth rate (RGR) after removal of extra water by paper towel.

The calculation formula was as follows [44]:

$$\text{RGR} = (\ln w_2 - \ln w_1) / \Delta t$$

where  $w_1$  was wet weight 1, which referred to the initial wet weight of the thalli, and  $w_2$  represented wet weight 2, which referred to the wet weight after culture at a specific temperature.  $\Delta t$  referred to the time between cultures, i.e., 5 days.

### 2.3. Protoplast Isolation, Fluorescent Brightener 28 and Evans Blue Staining

About 0.5 g of the *N. yezoensis* gametophyte blades were cleaned with 0.7% KI for 10 min and cut into 2 mm<sup>2</sup> fragments in enzyme solution composed of 150  $\mu\text{L}$  of abalone enzyme (crude extract was obtained directly from abalone, after centrifugation at 12,000  $\times g$  for 10 min at 4 °C to remove the insoluble materials) and 2 mL of seawater [45,46]. After digesting at room temperature for 4 h, the disintegration of single cells and protoplasts could be observed under a microscope. Thereafter, protoplasts were collected by centrifugation and diluted to a proper concentration, then cultured in sterilized seawater in light incubators at 13 °C, 17 °C, 21 °C, and 25 °C, respectively. The absence of cell wall from the isolated protoplasts was confirmed by staining with 0.1% Calcofluor White M2R

(Fluorescentbrightener28, Sigma, St. Louis, MO, USA) under a UV fluorescence microscope (Leica, DM2500, Wetzlar, Germany). To determine the viability of protoplasts, 0.5% Evans blue staining solution was added and incubated for 5 min at room temperature before observation under a microscope. Dead cells were dyed blue. Therefore, the survival rate of protoplasts was obtained by calculating the proportion of unstained living protoplasts in the total number of protoplasts. To assess the effects of ERK on the survival and regeneration of protoplasts, 10  $\mu$ M FR 180204 (ERK inhibitor) was applied to the culture medium at 13 °C for 10 days [47]. The survival rate was measured as described above and the division rate was calculated as the proportion of dividing cells in the total number of cells.

#### 2.4. DNA Extraction and Gene Cloning

Total DNA was extracted by using NuClean Plant Genomic DNA Kit (CWBI, Shanghai, China). The primers were designed by Primer-blast (<https://www.ncbi.nlm.nih.gov/tools/primer-blast/> accessed on 2 March 2021) in National Center for Biotechnology Information (NCBI) database (<https://www.ncbi.nlm.nih.gov> accessed on 2 March 2021). PCR amplification of Cyclin B was conducted at 94 °C for 10 min and 30 cycles (94 °C for 30 s, 55 °C for 30 s, and 72 °C for 30 s); amplification of CDKB was conducted at 94 °C for 10 min and 30 cycles (94 °C for 30 s, 55 °C for 30 s, and 72 °C for 60 s), followed by an extension reaction at 72 °C for 7 min. PCR products were purified in 1% agarose gel, and the target fragment was excised and cloned into a pESI-T vector (Yeasen, Shanghai, China). After transforming the fragments into competent *Escherichia coli* cells, positive recombinants were identified and sequenced for verification (Invitrogen, Shanghai, China).

The Cyclin B and CDKB gene sequences were analyzed using the BLAST algorithm available at the NCBI website. MEGA5 software was used to compare the protein coding sequences of Cyclin B and CDKB in *N. yezoensis* with the amino acid sequences of similar sequence information obtained from BLAST in NCBI. The neighbor joining (NJ) method was used and phylogenetic evolutionary tree including Cyclin B and CDKB were constructed, respectively.

#### 2.5. Determination of Photosynthetic Pigments Content

After incubation at different temperatures for 2 d, 4 d, and 6 d, fresh thalli of *N. yezoensis* were taken out to analyze its content of photosynthetic pigments. After absorbing extra water with paper towel, 0.1 g of samples were weighed and fully ground in liquid nitrogen. Then, 1 mL of 100% methanol was added to extract pigments at 4 °C for 24 h. After centrifuging for 10 min at 4 °C, 5000  $\times$  g, Chl *a* (652 and 665 nm) and carotenoids (480 and 510 nm) were obtained from the supernatant, the concentrations of which were determined by fluorescence photometer [48].

After fully grinding 0.1 g of thalli in liquid nitrogen, 1 mL of 0.05 mol/L phosphate buffer (pH = 6.8) was added to extract phycobiliproteins. The extract was kept at room temperature for 3 min and then frozen at  $-20$  °C for 30 min, after then, the extract was taken out and kept at room temperature for 1 h before frozen again. Repeated thawing and freezing for more than 3 times. Phycoerythrin (PE) and phycocyanin (PC) were obtained by collecting the supernatant after centrifuging for 10 min at 4 °C, 3500  $\times$  g. The concentrations of PE (455, 564, and 592 nm) and PC (592, 618, and 645 nm) were determined by fluorescence photometer [49].

#### 2.6. Quantification of Gene Expression by RT-qPCR

Thalli cultured at different temperatures were collected after 6, 12, 24, and 72 h incubation. Total RNA was isolated by using RNAPure Plant Kit (DNase I) (CWBI, Shanghai, China), and cDNA was synthesized by using Hifair<sup>®</sup>III1st Strand cDNA Synthesis Kit (YEASEN, Shanghai, China) according to the manufacturer's instructions. The primers for the quantification of gene expression (cyclin B-qF: TCATTGACCGGTTCCCTCTCC; cyclin B-qR: CGGGTCTCAGGAGCGTAGAT) were designed by using Primer-blast ([https://www.ncbi.nlm.nih.gov/tools/primer-blast/index.cgi?LINK\\_LOC=BlastHome](https://www.ncbi.nlm.nih.gov/tools/primer-blast/index.cgi?LINK_LOC=BlastHome) accessed

on 5 July 2021) in NCBI. The  $2^{-\Delta\Delta ct}$  method was used to quantify the transcription at different temperatures after normalization to actin, and the relative expression level of Cyclin B was calculated as fold change of transcription at 13 °C.

### 2.7. Protein Extraction and Western Blot Analysis

Thalli cultured at different temperatures were collected after 6, 12, 24, and 72 h incubation. The total proteins were extracted by using plant protein extraction kit (CW BIO, Shanghai, China), and their concentration was determined by using BCA Protein Assay Kit (CW BIO, Shanghai, China).

By using SDS-PAGE Gel Quick preparation Kit (Beyotime, Shanghai, China), the 12% SDS-polyacrylamide gels were prepared. Protein samples were boiled at 100 °C for 5 min, and then loaded with 20 µg of total protein per lane. After performing electrophoresis for 30 min at 70 V, the electrophoresis condition was changed to 120 V for 90 min. The protein was finally transferred onto polyvinylidene fluoride membranes (Millipore, Billerica, MA, USA). The membranes were blocked with 5% non-fat milk diluted in TBST (TBS with Tween-20) for 90 min at room temperature. After washing the sample thrice with TBST for 10 min sequentially, we incubated the membranes with the following antibodies: Phospho-p44/42 MAPK (Erk1/2) (Thr202/Tyr204) (D13.14.4E) XP<sup>®</sup> Rabbit mAb (dilution, 1/2000; Cell Signaling Technology, Danvers, MA, USA), p44/42 MAPK (Erk1/2) antibody (dilution, 1/2000; Cell Signaling Technology, Danvers, MA, USA), β-actin antibody (dilution, 1/2500; PhytoAB, San Francisco, CA, USA); CYCB1-1 antibody (dilution, 1/2000; orb28110, biorbyt, Cambridge, UK) overnight (at least for 16 h) at 4 °C. The sample was washed again thrice and incubated with secondary antibody: horseradish peroxidase (HRP)-conjugated affinipure goat anti-Rabbit IgG(H+L) (Proteintech) for 70 min at room temperature. The proteins were detected by enhanced chemiluminescence reagents (Thermo Fisher Scientific, MA, USA) and were analyzed using Image J (National Institute of Health, Bethesda, MD, USA), with β-actin as internal control.

### 2.8. Statistical Analysis

Results of all the experiments were expressed as the means ± standard deviation, and data were analyzed using 2-way ANOVA Multiple comparisons. Parameter estimates were examined using Tukey's test. All statistical analyses were conducted using GraphPad Prism software (<https://www.graphpad.com/scientific-software/prism/> accessed on 22 August 2021 and 9 April 2022).

## 3. Results

### 3.1. The Increase in Temperature Had a Negative Effect on the Growth of *N. yezoensis*

#### 3.1.1. The Increase in Temperature Reduced the Relative Growth Rate of the Thalli of *N. yezoensis*

The relative growth rate of *N. yezoensis* decreased with the increase in temperature (Figure 1). In the four temperature conditions, the relative growth rate of *N. yezoensis* thalli was positive, indicating a normal growth state only at 13 °C; in contrast, the relative growth rates were all negative at 17 °C, 21 °C, and 25 °C, indicating that higher temperature had a kind of inhibition effect on the growth of *N. yezoensis*. Therefore, 13 °C was the suitable temperature for *N. yezoensis* growth; a higher temperature inhibits the growth, exhibiting a kind of stress.

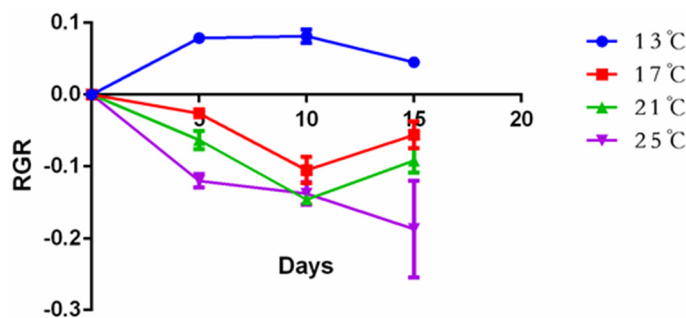


Figure 1. The relative growth rates of *N. yezoensis* thalli at different temperatures.

### 3.1.2. The Increase in Temperature Changed the Contents of Phycobiliprotein and Photosynthetic Pigment

The contents of phycocyanin and phycoerythrin at 13 °C and 17 °C remained relatively stable with a slight change over time, and the variation trends closely resembled each other; however, when cultured at higher temperatures of 21 °C and 25 °C, the contents of phycocyanin and phycoerythrin significantly increased after incubation over 4 days, and were much higher than that at 13 °C (Figure 2a,b). The contents of Chl *a* and carotenoid increased within 2 days at all groups, which was 2 days earlier than that of phycobiliprotein, then they significantly decreased after 2 days at 21 °C and 25 °C (Figure 2c,d). The losses of Chl *a* and carotenoids indicated the damage to the photosynthetic apparatus, while the high expression of phycobilin meant the activation of antioxidant system of the algae to cope with stress [17], suggesting that high temperature caused damage to algal photosystem, which further inhibited their normal growth. Therefore, from the perspective of changes in photosynthetic pigment content, thalli can maintain normal physiological state at 13–17 °C.

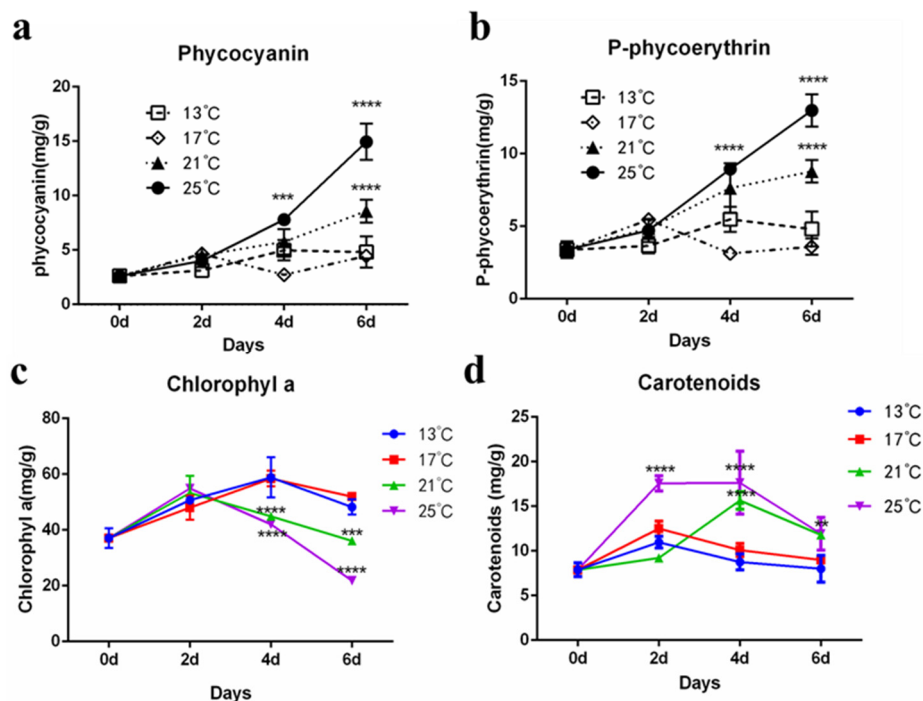
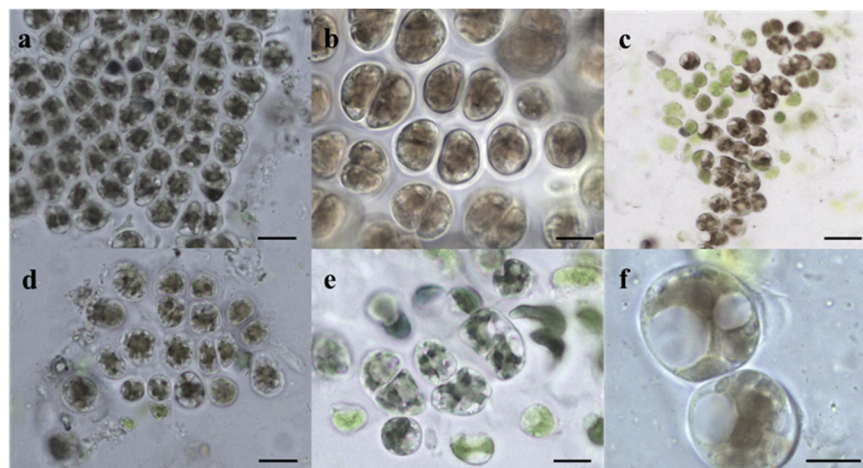


Figure 2. Changes of pigment contents in *N. yezoensis* incubated at different temperatures. (a,b): the content of phycoerythrin and phycocyanin; (c,d): the content of Chl *a* and Car; 0 d represented incubation of the algae at different temperatures for 4 h. Data represent mean  $\pm$  standard errors ( $n = 3$ ). \*\*  $p < 0.01$ , \*\*\*  $p < 0.001$ , \*\*\*\*  $p < 0.0001$ , vs. 13 °C.

### 3.1.3. High Temperature Inhibited the Survival and Division of Protoplasts

Protoplasts were isolated from the gametophyte blades of *N. yezoensis* by enzymatic hydrolysis. As shown in Figure 3, under the action of enzymatic hydrolysate, the cell wall gradually disintegrated, the interaction between cells was gradually “cut off”, and the gap between cells became larger (Figure 3a–e). Finally, single isolated protoplasts were obtained by centrifugation, and the diameter of protoplasts ranged from 10 to 20  $\mu\text{m}$  (Figure 3f). At the cutting surface caused by scissors, the cell wall was relatively weak and easy to be enzymatically hydrolyzed, resulting in more cell rupture and pigment leakage (Figure 3c).



**Figure 3.** Enzymatic hydrolysis process of *N. yezoensis* and the isolated protoplasts (a–e): the enzymatic hydrolysis process enlarged the gaps between algal cells (scale bar = 20  $\mu\text{m}$ ); (f): single protoplast (scale bar = 10  $\mu\text{m}$ ).

Cell fragments generated during the preparation of protoplasts by scissor shearing and enzymatic hydrolysis no longer had intact cell membranes and thus were stained blue after incubation with Evans blue dye, while protoplasts with intact cell membrane remained unstained because of the membrane’s selective permeability of the dye, making the dead and intact alive protoplasts distinguishable from each other (Figure 4).

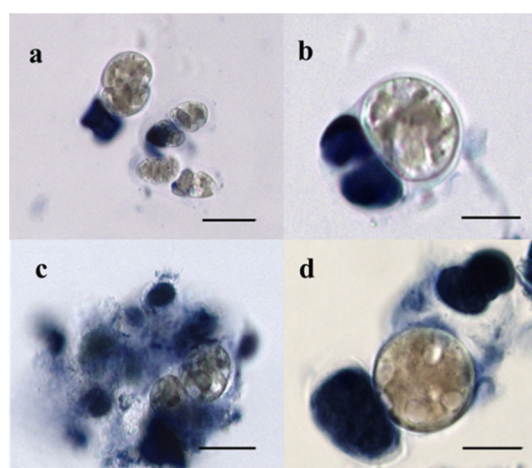


**Figure 4.** Detection of protoplasts by Evans blue staining. Dead protoplasts or cell fragments were stained by Evans blue. The survival rate of protoplasts was determined after Evans blue staining. (a,c): Scale bar = 20  $\mu\text{m}$ ; (b,d): Scale bar = 10  $\mu\text{m}$ .

Regeneration of the cell wall of protoplasts could be observed in 2 days by FB28 staining in blue under UV fluorescence microscope (Figure 5). The regeneration of cell wall

in protoplasts indicated that the cells were in a normal state and could continue to grow and divide.

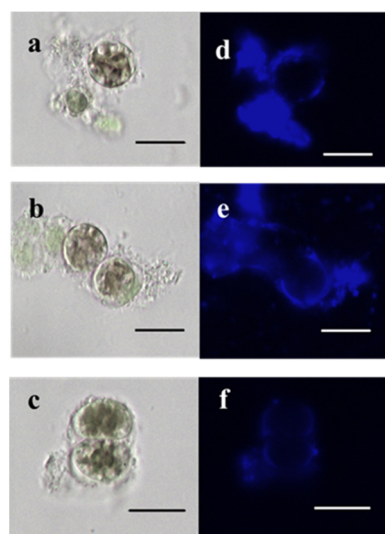


**Figure 5.** Confirmation of cell wall regeneration by FB28 staining. After incubation for 2 days, protoplasts (a–c) were stained with FB 28. The presence of regenerated cell wall (in blue) was confirmed under UV fluorescence microscope (d–f). Scale bars = 20  $\mu\text{m}$ .

After incubation at different temperatures for certain time, the protoplasts were stained with Evans blue dye, and the dead and intact alive cells were counted under a microscope. The results showed that the survival rate of protoplasts decreased with the increase in temperature, especially in the treatment group of 25 °C. After 4 days, the survival rate of protoplasts decreased obviously, and by the 10th day, all protoplasts cultivated at 25 °C died (Table 1). Regarding protoplast division, incubation at high temperature showed inhibition effect on it. As shown in Figure 6 and Table 1, cell division was observed in all the protoplasts incubated at temperatures except for 25 °C, and the division rate of protoplasts cultured at 13 °C and 17 °C, which was considered to be the suitable temperature range for algal growth, maintained high in the first few days; however, the ratio of divided cells to the total cells decreased with the increase in culture temperature (Table 1).

**Table 1.** Survival rates and division rates of protoplasts incubated at different temperatures.

Temperature	Survival Rates of Protoplasts					Division Rates of Protoplasts		
	2 Days	4 Days	6 Days	8 Days	10 Days	2 Days	4 Days	6 Days
13 °C	98% $\pm$ 2%	80% $\pm$ 1%	76% $\pm$ 1%	69% $\pm$ 1%	52% $\pm$ 2%	12% $\pm$ 1%	47% $\pm$ 1%	67% $\pm$ 1%
17 °C	98% $\pm$ 1%	76% $\pm$ 3%	70% $\pm$ 1%	63% $\pm$ 2%	49% $\pm$ 1%	9% $\pm$ 1%	34% $\pm$ 1%	51% $\pm$ 2%
21 °C	94% $\pm$ 2%	69% $\pm$ 1%	63% $\pm$ 1%	56% $\pm$ 1%	41% $\pm$ 1%	7%	23% $\pm$ 3%	34% $\pm$ 1%
25 °C	44% $\pm$ 1%	15% $\pm$ 1%	6% $\pm$ 3%	3% $\pm$ 1%	0	0	0	0

### 3.2. Clone and Sequence Analysis of Cyclin B, CDKB

Based on our previous transcriptome data of *N. yezoensis* (not yet published), partial coding sequence (CDS) of Cyclin B and complete CDS of CDKB were successfully cloned. Sequences have been uploaded to NCBI, and Genbank numbers were OM320797 and OM320799, respectively. The phylogenetic tree displayed phylogenetic positions of these genes: Cyclin B was clustered into one subgroup cloned from *Pycnococcus provasolii*, *Trebouxia sp.*, *Chlorella sorokiniana*, *Ostreococcus tauri*, *Dunaliella salina*, *Raphidocelis subcapitata*, and *Monoraphidium neglectum*, respectively, and an adjacent subgroup from *Gonium pectorale*, *Tetrabaena socialis*, and *Volvox carteri f. nagariensis* (Supplementary Materials Figure S1c). CDKB was clustered into one subgroup from *Chondrus crispus*, *Gracilariaopsis chorda*, *Cyanidioschyzon merolae*, and *Porphyridium purpureum*, respectively, and an adjacent subgroup from

*Elaeis guineensis*, *Phoenix dactylifera*, *Dioscorea cayenensis* subsp. *rotundata*, *Sorghum bicolor*, *Zingiber officinale*, and *Solanum lycopersicum* (Figure S1d).

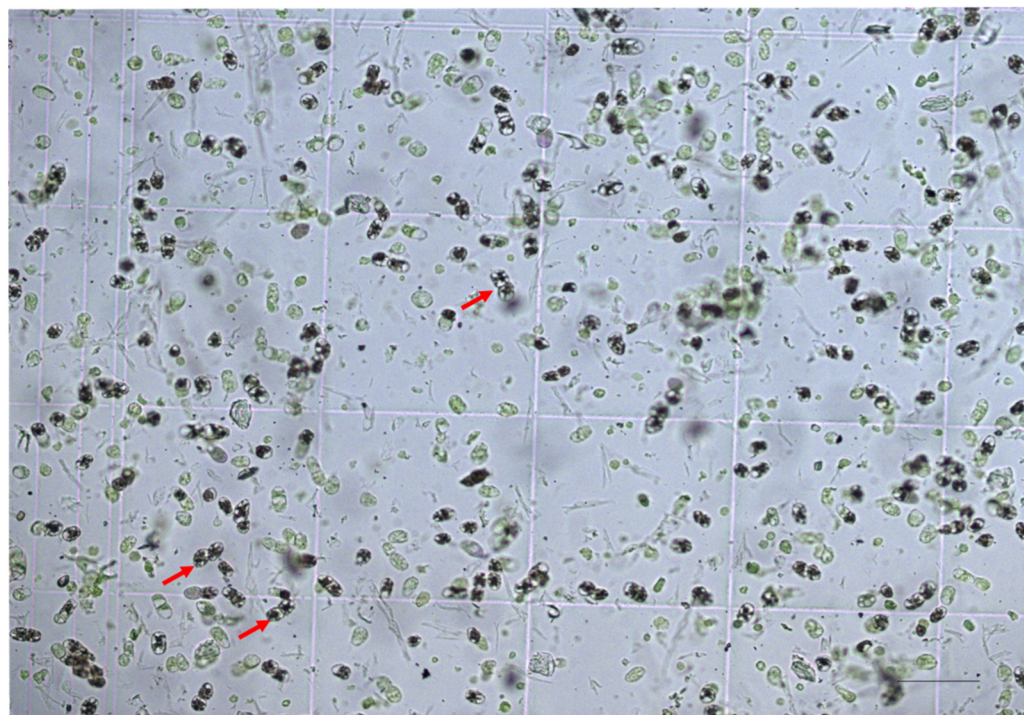


**Figure 6.** Microscopic observation of protoplasts culture by hemocytometer. The red and brown cells were normal, and the green fragments were dead. The red arrows denoted the representative division cells (Scale bars = 100  $\mu\text{m}$ ).

### 3.3. The Relative Expression Level of Cyclin B in *N. yezoensis* at Different Temperatures

Since the expression of Cyclin B changes periodically during the process of cell cycle, leading to CDK activation/ inhibition and the progression of cell cycle and cell division, the expression of Cyclin B in *N. yezoensis* was studied to determine whether it was involved in algal growth in response to high temperature stress of 17 °C, 21 °C, and 25 °C, comparing to the normal control of 13 °C. The results showed that, the transcription level of Cyclin B was strongly upregulated with the increase in temperature at 6 h; the higher the temperature, the greater the level of such upregulation (Figure 7). However, prolonged high temperature stress gradually diminished its effect on upregulating Cyclin B transcription; at 48 h, the relative expression level of Cyclin B at 25 °C was lower than that at 13 °C (Figure 7), suggesting that high temperature stress inhibits the transcription of Cyclin B over time.

Western blot results showed that the protein level of Cyclin B increased significantly with the increase in temperature at 12 h, and reached a level of nearly 10 folds of actin control at 25 °C (Figure 8a); however, incubation at high temperatures for 72 h decreased the protein level of Cyclin B, and the level of which at 25 °C was significantly lower than that at 13 °C ( $p < 0.01$ , Figure 8b), suggesting that high temperature stress downregulates Cyclin B over time.

Taken together, the above studies demonstrated that short-term (within 12 h in this study) heat stress stimulated the expression of Cyclin B, while long-term heat stress significantly downregulated it, which may lead to the arrest of cell cycle progression and inhibition of cell division.

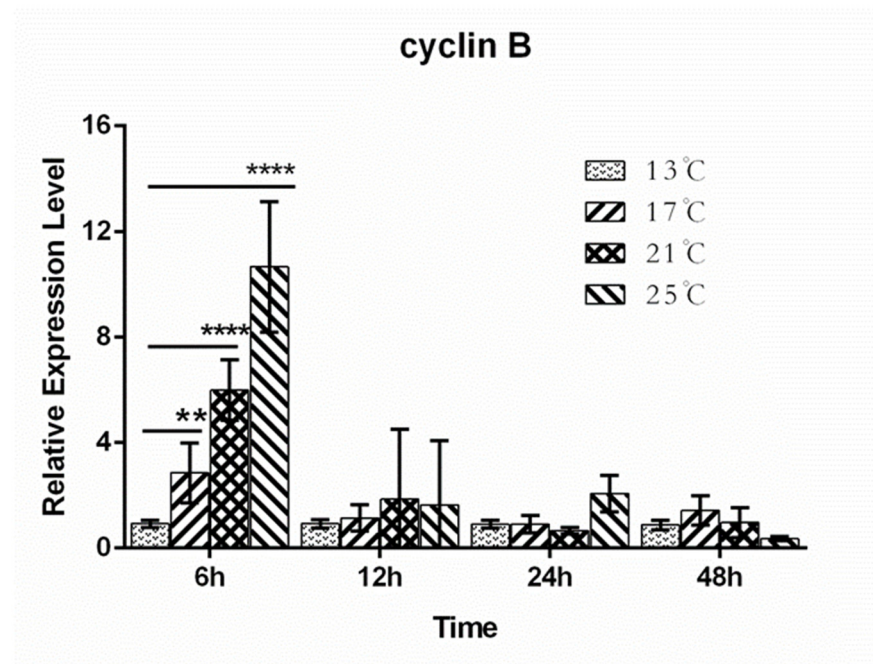


**Figure 7.** The relative expression level of Cyclin B in *N. yezoensis* incubated at different temperatures. Data represent mean ± standard errors ( $n = 3$ ). \*\*  $p < 0.01$ , \*\*\*\*  $p < 0.0001$ , vs. 13 °C.

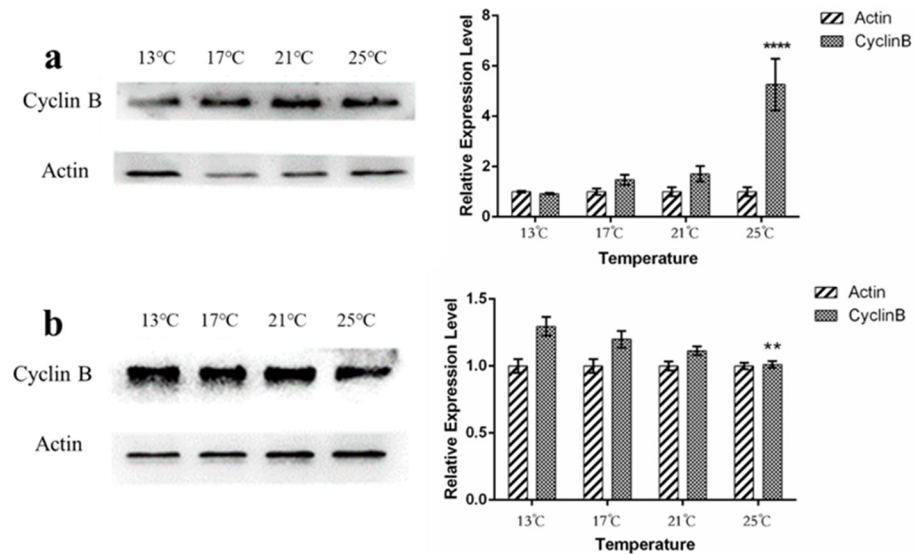


**Figure 8.** The protein level of Cyclin B in *N. yezoensis* incubated at different temperatures: (a) the expression of Cyclin B increased with the increase in temperature at 12 h; (b) the expression of Cyclin B decreased with the increase in temperature at 72 h. Data represent mean ± standard errors ( $n = 3$ ). \*\*  $p < 0.01$ , \*\*\*\*  $p < 0.0001$ , vs. 13 °C.

### 3.4. The ERK Signaling Pathway Involved in the Response of *N. yezoensis* to Temperature Changes

Studies have shown that ERK signaling pathway regulates cell division. In this study, we found that the phosphorylation level of ERK, which represented the activity level of ERK signaling pathway, decreased with the increasing temperature after the thalli cultured at different temperatures for 48 h, indicating that high temperature stress inhibits the activation of ERK signaling pathway. Thus, it can be speculated that cellular activities such as division, growth, and development responses downstream of ERK signaling pathway are also inhibited by high temperature stress (Figure 9).

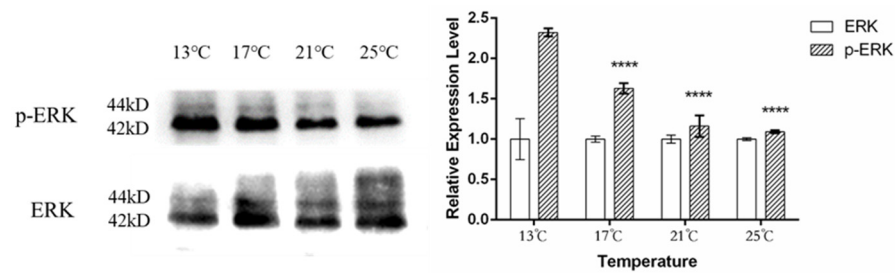


**Figure 9.** The phosphorylation of ERK decreased with an increase in temperature at 48 h. Data represent mean  $\pm$  standard errors ( $n = 3$ ). \*\*\*\*  $p < 0.0001$ , vs. 13 °C.

To verify the involvement of ERK signaling pathway in cellular functions of *N. yezoensis*, we added the ERK inhibitor FR 180204 to the seawater in which the protoplasts were cultured at 13 °C. Within 4 days, the addition of inhibitor FR 180204 significantly reduced the survival rate of protoplasts ( $p < 0.05$ ); and it continued to decrease over time (Figure 10a). Moreover, cell division was inhibited by the ERK inhibitor, as shown in Figure 10b that the division rates of protoplasts were significantly lower with the existence of FR 180204 ( $p < 0.01$ ).

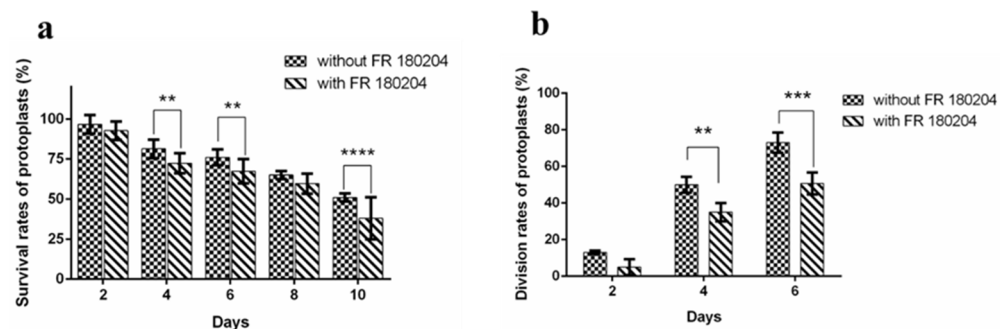


**Figure 10.** Effects of ERK inhibitor FR 180204 on the survival and division rates of protoplasts: (a) the changes of survival rates of protoplasts; (b) the changes of division rates of protoplasts. Data represent mean  $\pm$  standard errors ( $n = 3$ ). \*\*  $p < 0.01$ , \*\*\*  $p < 0.001$ , \*\*\*\*  $p < 0.0001$ , vs. without FR 180204.

#### 4. Discussion

Temperature has been reported to greatly affect the growth and development of *N. yezoensis*. Repeated rises in temperature from 18 °C to 23 °C and 24 °C inhibited the development of *N. yezoensis* germlings, resulting in large-scale rotting of blades, and consequently a sharp drop of the yield [43]. The gametophyte thalli of *N. yezoensis* on the cultivation rafts located in the offshore farm grew very well at temperatures between 10 and 15 °C [41]; when the temperature was higher than that, the thalli exhibited retarded growth and the yield decreased [24]. This was consistent with the results of this study: only thalli incubated at 13 °C maintained a net increase in relative growth rate, while those incubated at 17 °C and higher temperatures showed a loss of weight (Figure 1); protoplasts cultured at 13 °C got a much higher survival rate and regeneration rate than those at 17 °C and higher temperatures (Table 1). However, in the outdoor raceway tanks with circulating water, the optimum seawater temperature for the growth of *N. yezoensis* thalli ranged from 10 to 17 °C, which was higher than that in Nori cultivation farm [50]; the difference may partly be a reflection of the condition that the seawater temperature in Nori cultivation farm does not change independently but changes along with other factors. The above results indicate that temperature over 17 °C may lead to heat stress of *N. yezoensis*, thereby negatively affecting algal growth and development.

The composition and contents of photosynthetic pigments in *N. yezoensis*, which closely correlate to the photosynthetic rate and the quality of plant and algal products, will

fluctuate in response to environmental stress [19]. *Meristotheca papulose*, a subtidal red alga that grows in an ambient temperature of 20 °C, was reported to reach the highest level of its maximum net photosynthetic rate (NP<sub>max</sub>) and high saturation light intensity when incubated over-night (12 h) at 28 °C, and the lowest level at 12 °C [20]. The photosynthetic pigment ratios of *N. yezoensis* increased with the increase in temperature [13]. When *Geitlerinema amphibium* (BA-13), mat-forming cyano-bacterium from the southern Baltic Sea, was cultured at three temperatures (15 °C, 22.5 °C, and 30 °C), both Chl *a* and β-carotene increased slightly with the increase in temperature [22]. In this study, compared with the control group (13 °C), heat stress (temperatures above 17 °C) increased the contents of phycobiliproteins but decreased the contents of Chl *a* and carotenoids (Figure 2), which was consistent with Li et al. in *Gelidium amansii* [17]. Taking the most suitable temperature (20 °C) for photosynthesis of *Gelidium amansii* as control, the content of phycobiliproteins, which has been proven that can effectively resist oxidative stress [51], increased when the thalli were treated at 30 °C for 12 h and longer, suggesting that phycobiliproteins were upregulated to alleviate oxidative damage in response to heat stress. Therefore, it can be speculated that the upregulation of phycobiliproteins in *N. yezoensis* in this study served as a part of the activated antioxidant system in response to high temperature stress. Furthermore, high temperatures led to a significant decrease in photosynthetic pigments Chl *a* and carotenoids over time, suggesting the destroyed photosynthetic system of the algae by sustained exposure to heat stress.

Heat stress has been reported to affect cell cycle progression. Synchronized *Tobacco* BY-2 cells were transiently arrested at G1/S or G2/M when exposed to heat stress (30 °C) at late/early G1 stage. Slowing down of cell cycle progression was associated with transient delays in expression of A-, B-, and D-type cyclins, such as Ntcyc29 (a cyclin B gene) and CycD3-1 [52]. In *Chlamydomonas*, there is only one type Cyclin (CYCB1); the cycb1-5 mutation (p. Glu325 > Lys) caused a strong temperature-sensitive lethal phenotype, and mutant cells were arrested after one round of replication and exhibited aberrant initiation of cytokinesis at approximately the same time that wild-type cells performed their first complete cell division at the restrictive temperature (33 °C) [34]. In this study, high temperature stress significantly affected the expression of Cyclin B, with short-term treatment upregulating its transcription (6 h) and protein level (12 h), while long-term treatment reduced its protein level (72 h, Figure 8). As is well known, CDK activity greatly depends on its association with Cyclin B; lower level of Cyclin B results in less activation of CDK, and thereafter arrest of cell cycle progression and inhibition of cell division. Therefore, long-term high temperature stress in this study may inhibit protoplast division of *N. yezoensis* (Table 1) by downregulating Cyclin B. However, high temperature can also lead to cell cycle arrest at high mitotic CDK activity as reported in *Chlamydomonas reinhardtii*, which decreased after transfer to normal culture temperature to complete nuclear and cell division, suggesting that blocking of processes at downstream of CDK rather than CDK itself mediates the cell cycle arrest at high temperature [31]. In this study, whether the upregulation of Cyclin B protein expression detected in the thalli after 12 h incubation at high temperatures (17 °C, 21 °C, 25 °C) promotes cell cycle progression requires further verification. Interestingly, some studies have shown that in *Euglena* it is possible to synchronize the division cycle and the growth cycle by heat shocks [53], and the inhibition of mitosis by repetitive heat treatment (34 °C and 35 °C) may be due to the irreversible denaturation of the enzyme system required for mitosis.

The cell cycle is a key part of plant growth and MAPKs have been shown to play a central role in the control of cell cycle. Studies have demonstrated the role of MAPKs in response to temperature stress [54]. In rice, temperature changes affected the transcription of OsMSRMK2 (a rice MAPK gene); high temperature (37 °C) treatment for 30 min significantly decreased its transcription, while treatment at 25 °C for 30 min significantly increased its transcription [55]. A total of 15 MAPKs have already been identified from *N. yezoensis* (PyMAPKs) [56], but their function analysis has not been studied. In this study, it was found that high temperature stress significantly inhibited the phosphorylation of ERK

in the thalli of *N. yezoensis* at 48 h and the phosphorylation level decreased with the increase in temperature (Figure 9). This was similar to the study in *Ulva rigida*; where ERK phosphorylation increased at increased temperature (+4 °C over ambient conditions) at 24 h, but decreased significantly after 72 h [57]. Elevated cadmium levels can trigger a wide range of cellular responses in plants, including changes in auxin and cell cycle-related gene expression and MAPKs play important roles in the signaling responses to heavy metal stress, auxin, and cell cycle cue. It was found that the disruption of the MAPK signaling pathway by inhibitor PD98059 significantly inhibited the root growth of cadmium-stressed rice, and the expression of the cell cycle-related gene was negatively regulated by MAPKs [58]. Further study revealed that exposure to ERK inhibitor decreased the survival and division rates of protoplasts isolated from the thalli of *N. yezoensis* (Figure 10). These results indicate that the ERK signaling pathway might be involved in *N. yezoensis*'s response to different temperatures; high temperature stress inhibits ERK activation and thus negatively regulates the viability, cell growth, and division process by downstream targets of ERK, but the specific regulatory network remains to be further studied.

**Supplementary Materials:** The following supporting information can be downloaded at: <https://www.mdpi.com/article/10.3390/w14142175/s1>, Figure S1. *N. yezoensis* Cyclin B and CDKB sequence analyses (a,b) and phylogenetic trees (c,d). a: DL500 marker (M) and the amplification of the partial coding sequence fragments of *Cyclin B* (1); b: DL2000 marker (M) and the amplification of the complete *CDKB* (2); c,d: the phylogenetic trees of *Cyclin B* and *CDKB*.

**Author Contributions:** J.Y.: methodology, formal analysis, investigation, writing—original draft preparation; A.L.: investigation, experiment condition exploration, formal analysis; T.C.: visualization; L.H.: validation, supervision; S.S.: conceptualization, visualization, funding acquisition. All authors have read and agreed to the published version of the manuscript.

**Funding:** This research was funded by the National Key R & D Program of China, grant number “2018YFD0901500”, and the Project Funded by the Priority Academic Program Development of Jiangsu Higher Education Institutions (PAPD).

**Institutional Review Board Statement:** Not applicable.

**Informed Consent Statement:** Not applicable.

**Data Availability Statement:** The sequence information has been submitted to NCBI. Genbank numbers are OM320797 and OM320799.

**Conflicts of Interest:** The authors declare that they have no conflict of interest to this work. We declare that we do not have any commercial or associative interest that represents a conflict of interest in connection with the work submitted.

## References

1. Ding, H.C.; Yan, X.H. Advances in *Pyropia* (formerly *Porphyra*) genetics and breeding. *J. Fish. Sci. China* **2019**, *26*, 592. [CrossRef]
2. Cho, T.J.; Rhee, M.S. Health Functionality and Quality Control of Laver (*Porphyra*, *Pyropia*): Current Issues and Future Perspectives as an Edible Seaweed. *Mar. Drugs* **2019**, *18*, 14. [CrossRef] [PubMed]
3. Sasuga, K.; Yamanashi, T.; Nakayama, S.; Ono, S.; Mikami, K. Discolored red seaweed *Pyropia yezoensis* with low commercial value Is a novel resource for production of agar polysaccharides. *Mar. Biotechnol.* **2018**, *20*, 520–530. [CrossRef] [PubMed]
4. Chen, N.C.; Tang, L.; Guan, X.W.; Chen, R.; Cao, M.; Mao, Y.X.; Wang, D.M. Thallus sectioning as an efficient monospore release method in *Pyropia yezoensis* (Bangiales, Rhodophyta). *J. Appl. Phycol.* **2020**, *32*, 2195–2200. [CrossRef]
5. Wells, M.L.; Potin, P.; Craigie, J.S.; Raven, J.A.; Merchant, S.S.; Helliwell, K.E.; Smith, A.G.; Camire, M.E.; Brawley, S.H. Algae as nutritional and functional food sources: Revisiting our understanding. *J. Appl. Phycol.* **2017**, *29*, 949–982. [CrossRef]
6. Tseng, C.K.; Chang, T.J. Studies on *Porphyra*I. life history of *Porphyra tenera* kjellm. *Bull. Bot.* **1954**, *3*, 287–302.
7. Gao, D.; Kong, F.; Sun, P.P.; Bi, G.Q.; Mao, Y.X. Transcriptome-Wide identification of optimal reference genes for expression analysis of *Pyropia yezoensis* responses to abiotic stress. *BMC Genom.* **2018**, *19*, 251. [CrossRef]
8. Singh, S.P.; Singh, P. Effect of temperature and light on the growth of algae species: A review. *Renew. Sustain. Energy Rev.* **2015**, *50*, 431–444. [CrossRef]
9. Zhang, C.C.; Wei, H.; Song, G.S.; Xie, C. IPCC-CMIP5 based projection and analysis of future sea surface temperature changes in coastal seas east of China. *J. Oceanol. Limnol.* **2020**, *51*, 1288–1300.

10. Tulandi, D.A.; Tumangkeng, J.V. Analysis of daily dynamics of thermal interaction of temperature and ocean flow in seaweed growth areas. *J. Phys. Conf. Ser.* **2021**, *1968*, 012035. [[CrossRef](#)]
11. Le, B.; Nadeem, M.; Yang, S.-H.; Shin, J.-A.; Kang, M.-G.; Chung, G.; Sun, S.M. Effect of silicon in *Pyropia yezoensis* under temperature and irradiance stresses through antioxidant gene expression. *J. Appl. Phycol.* **2018**, *31*, 1297–1302. [[CrossRef](#)]
12. Kakinuma, M.; Coury, D.A.; Nakamoto, C.; Sakaguchi, K.; Amano, H. Molecular analysis of physiological responses to changes in nitrogen in a marine macroalga, *Porphyra yezoensis* (Rhodophyta). *Cell Biol. Toxicol.* **2008**, *24*, 629–639. [[CrossRef](#)] [[PubMed](#)]
13. Zhang, T.; Li, J.F.; Ma, F.; Lu, Q.Q.; Shen, Z.G.; Zhu, J.Y. Study of photosynthetic characteristics of the *Pyropia yezoensis* thallus during the cultivation process. *J. Appl. Phycol.* **2014**, *26*, 859–865. [[CrossRef](#)]
14. Wang, H.Z.; Yan, X.H.; Li, L. Isolation and characterization of high-temperature resistant strains of *Porphyra yezoensis* Ueda (Bangiales, Rhodophyta). *J. Oceanol. Limnol.* **2012**, *43*, 363–369.
15. Wu, H.H.; Ding, H.C.; Yan, X.H. Selection and characterization of a high-temperature resistant strain by hybridization recombination in *Pyropia yezoensis*. *J. Fish. China* **2017**, *41*, 711–722.
16. Shin, Y.J.; Min, S.R.; Kang, D.Y.; Lim, J.M.; Park, E.J.; Hwang, M.S.; Choi, D.W.; Ahn, J.W.; Park, Y.; Jeong, W.J.; et al. Characterization of high temperature-tolerant strains of *Pyropia yezoensis*. *Plant Biotechnol. Rep.* **2018**, *12*, 365–373. [[CrossRef](#)]
17. Li, Y.F.; Liu, J.G.; Zhang, L.T.; Pang, T.; Qin, R.Y. Effects of temperature on the photosynthetic performance in mature thalli of the red alga *Gelidium amansii* (Gelidiaceae). *Aquaculture* **2019**, *512*, 734320. [[CrossRef](#)]
18. Sekar, S.; Chandramohan, M. Phycobiliproteins as a commodity: Trends in applied research, patents and commercialization. *J. Appl. Phycol.* **2008**, *20*, 113–136. [[CrossRef](#)]
19. Zhang, T.; Shen, Z.G.; Xu, P.; Zhu, Z.Y.; Lu, Q.Q.; Shen, Y.; Wang, Y.; Yao, C.Y.; Li, J.F.; Wang, Y.X.; et al. Analysis of photosynthetic pigments and chlorophyll fluorescence characteristics of different strains of *Porphyra yezoensis*. *J. Appl. Phycol.* **2012**, *24*, 881–886. [[CrossRef](#)]
20. Borlongan, I.A.; Suzuki, S.; Nishihara, G.N.; Kozono, J.; Terada, R. Effects of light quality and temperature on the photosynthesis and pigment content of a subtidal edible red alga *Meristotheca papulosa* (Solieriaceae, Gigartinales) from Japan. *J. Appl. Phycol.* **2020**, *32*, 1329–1340. [[CrossRef](#)]
21. Markovic, S.M.; Zivancev, D.; Horvat, D.; Torbica, A.; Jovankic, J.; Djukic, N.H. Correlation of elongation factor 1A accumulation with photosynthetic pigment content and yield in winter wheat varieties under heat stress conditions. *Plant Physiol. Biochem.* **2021**, *166*, 572–581. [[CrossRef](#)] [[PubMed](#)]
22. Jodłowska, S.; Latała, A. Combined effects of light and temperature on growth, photosynthesis, and pigment content in the mat-forming cyanobacterium *Geitlerinema amphibium*. *Photosynthetica* **2013**, *51*, 202–214. [[CrossRef](#)]
23. Watanabe, Y.; Nishihara, G.N.; Tokunaga, S.; Terada, R. Effect of irradiance and temperature on the photosynthesis of a cultivated red alga, *Pyropia tenera* (= *Porphyra tenera*), at the southern limit of distribution in Japan. *Phycol. Res.* **2014**, *62*, 187–196. [[CrossRef](#)]
24. Takahashi, M.; Kumari, P.; Li, C.Z.; Mikami, K. Low temperature causes discoloration by repressing growth and nitrogen transporter gene expression in the edible red alga *Pyropia yezoensis*. *Mar. Environ. Res.* **2020**, *159*, 105004. [[CrossRef](#)]
25. Vitova, M.; Bisova, K.; Hlavova, M.; Kawano, S.; Zachleder, V.; Cizkova, M. *Chlamydomonas reinhardtii*: Duration of its cell cycle and phases at growth rates affected by temperature. *Planta* **2011**, *234*, 599–608. [[CrossRef](#)]
26. Björklund, M. Cell size homeostasis: Metabolic control of growth and cell division. *Biochim. Biophys. Acta—Mol. Cell Res.* **2018**, *1866*, 409–417. [[CrossRef](#)]
27. Oldenhof, H.; Zachleder, V.; van den Ende, H. Blue light delays commitment to cell division in *Chlamydomonas reinhardtii*. *Plant Biol.* **2004**, *6*, 689–695. [[CrossRef](#)]
28. Zachleder, V.; Ivanov, I.; Vitova, M.; Bisova, K. Effects of cyclin-dependent kinase activity on the coordination of growth and the cell cycle in green algae at different temperatures. *J. Exp. Bot.* **2018**, *70*, 845–858. [[CrossRef](#)]
29. Tobe, B.T.; Kitazono, A.A.; Garcia, J.S.; Gerber, R.A.; Bevis, B.J.; Choy, J.S.; Chasman, D.; Kron, S.J. Morphogenesis signaling components influence cell cycle regulation by cyclin dependent kinase. *Cell Div.* **2009**, *4*, 12. [[CrossRef](#)]
30. Čížková, M.; Pichová, A.; Vítová, M.; Pichová, M.; Pichová, J.; Umysová, D.; Gálová, E.; Seveovieva, A.; Zachleder, V.; Bisová, K. CDKA and CDKB kinases from *Chlamydomonas reinhardtii* are able to complement *cdc28* temperature-sensitive mutants of *Saccharomyces cerevisiae*. *Protoplasma* **2008**, *232*, 183–191. [[CrossRef](#)]
31. Zachleder, V.; Ivanov, I.; Vítová, M.; Bišová, K. Cell cycle arrest by supraoptimal temperature in the alga *Chlamydomonas reinhardtii*. *Cells* **2019**, *8*, 1237. [[CrossRef](#)] [[PubMed](#)]
32. Sasabe, M.; Machida, Y. Signaling Pathway that Controls Plant Cytokinesis. *Enzymes* **2014**, *35*, 145–165. [[PubMed](#)]
33. Tulin, F.; Cross, F.R. A microbial avenue to cell cycle control in the plant superkingdom. *Plant Cell* **2014**, *26*, 4019–4038. [[CrossRef](#)] [[PubMed](#)]
34. Atkins, K.C.; Cross, F.R. Interregulation of CDKA/CDK1 and the Plant-Specific Cyclin-Dependent Kinase CDKB in Control of the *Chlamydomonas* Cell Cycle. *Plant Cell* **2018**, *30*, 429–446. [[CrossRef](#)]
35. Wang, Z.; Wan, Y.Y.; Meng, X.J.; Zhang, X.L.; Yao, M.N.; Miu, W.J.; Zhu, D.M.; Yuan, D.S.; Lu, K.; Li, J.N.; et al. Genome-Wide identification and analysis of MKK and MAPK gene families in *Brassica* Species and response to stress in *Brassica napus*. *Int. J. Mol. Sci.* **2021**, *22*, 544. [[CrossRef](#)] [[PubMed](#)]
36. Chardin, C.; Schenk, S.T.; Hirt, H.; Colcombet, J.; Krapp, A. Review: Mitogen-Activated Protein Kinases in nutritional signaling in *Arabidopsis*. *Plant Sci.* **2017**, *260*, 101–108. [[CrossRef](#)]

37. Pitzschke, A.; Schikora, A.; Hirt, H. MAPK cascade signalling networks in plant defence. *Curr. Opin. Plant Biol.* **2009**, *12*, 421–426. [[CrossRef](#)]
38. Kalapos, B.; Hlavova, M.; Nadai, T.V.; Galiba, G.; Bisova, K.; Doczi, R. Early evolution of the Mitogen-Activated Protein Kinase Family in the plant Kingdom. *Sci. Rep.* **2019**, *9*, 4094. [[CrossRef](#)]
39. Lavoie, J.N.; L'Allemain, G.L.; Brunet, A.; Muller, R.; Pouyssegur, J. Cyclin D1 Expression Is Regulated Positively by the p42/p44MAPK and Negatively by the p38/HOGMAPK Pathway. *J. Biol. Chem.* **1996**, *271*, 20608–20616. [[CrossRef](#)]
40. Jimenez, C.; Cossio, B.R.; Rivard, C.J.; Berl, T.; Capasso, J.M. Cell division in the unicellular microalga *Dunaliella viridis* depends on phosphorylation of extracellular signal-regulated kinases (ERKs). *J. Exp. Bot.* **2007**, *58*, 1001–1011. [[CrossRef](#)]
41. Ma, J.; Xu, T.P.; Bao, M.L.; Zhou, H.M.; Zhang, T.Z.; Li, Z.Z.; Gao, G.; Li, X.S.; Xu, J.T. Response of the red algae *Pyropia yezoensis* grown at different light intensities to CO<sub>2</sub>-induced seawater acidification at different life cycle stages. *Algal Res.* **2020**, *49*, 101950. [[CrossRef](#)]
42. Zhang, B.L.; Yan, X.H.; Huang, L.B. Evaluation of an improved strain of *Porphyra yezoensis* Ueda (Bangiales, Rhodophyta) with high-temperature tolerance. *J. Appl. Phycol.* **2011**, *23*, 841–847. [[CrossRef](#)]
43. Ding, H.C.; Zhang, B.L.; Yan, X.H. Isolation and characterization of a heat-resistant strain with high yield of *Pyropia yezoensis* Ueda (Bangiales, Rhodophyta). *Aquac. Fish.* **2016**, *1*, 24–33. [[CrossRef](#)]
44. Hiraoka, M.; Oka, N. Tank cultivation of *Ulva prolifera* in deep seawater using a new “germling cluster” method. *J. Appl. Phycol.* **2007**, *20*, 97–102. [[CrossRef](#)]
45. Dipakkore, S.; Reddy, C.R.K.; Jha, B. Production and seeding of protoplasts of *Porphyra okhaensis* (Bangiales, Rhodophyta) in laboratory culture. *J. Appl. Phycol.* **2005**, *17*, 331–337. [[CrossRef](#)]
46. Dai, J.X.; Yang, Z.; Liu, W.S.; Bao, Z.M.; Han, B.Q.; Shen, S.S.; Zhou, L.R. Seedling production using enzymatically isolated thallus cells and its application in *Porphyra* cultivation. *Hydrobiologia* **2004**, *512*, 127–131. [[CrossRef](#)]
47. Yang, J.J.; Yin, Y.; Yu, D.C.; He, L.H.; Shen, S.D. Activation of MAPK signaling in response to nitrogen deficiency in *Ulva prolifera* (Chlorophyta). *Algal Res.* **2021**, *53*, 102153. [[CrossRef](#)]
48. Porra, R.J. The chequered history of the development and use of Simultaneous equations for the accurate determination of chlorophylls a and b. *Photosynth. Res.* **2002**, *73*, 149–156. [[CrossRef](#)]
49. Beer, S.; Eshel, A. Determining phycoerythrin and phycocyanin concentrations in aqueous crude extracts of red algae. *Mar. Freshw. Res.* **1985**, *36*, 785–792. [[CrossRef](#)]
50. Yamamoto, M.; Watanabe, Y.; Kinoshita, H. Effects of water temperature on the growth of red alga *Porphyra yezoensis* form. *narawaensis* (Nori) cultivated in an outdoor raceway tank. *Bull. Jpn. Soc. Sci. Fish.* **1991**, *57*, 2211–2217. [[CrossRef](#)]
51. Cano-Europa, E.; Ortiz-Butrón, R.; Gallardo-Casas, C.A.; Blas-Valdivia, V.; Pineda-Reynoso, M.; Olvera-Ramírez, R.; Franco-Colin, M. Phycobiliproteins from *Pseudanabaena tenuis* rich in c-phycoerythrin protect against HgCl<sub>2</sub>-caused oxidative stress and cellular damage in the kidney. *J. Appl. Phycol.* **2009**, *22*, 495–501. [[CrossRef](#)]
52. Jang, S.J.; Shin, S.H.; Yee, S.T.; Hwang, B.; Im, K.H.; Park, K.Y. Effects of abiotic stresses on cell cycle progression in *Tobacco* BY-2 Cells. *Mol. Cells* **2005**, *20*, 136–141. [[PubMed](#)]
53. Pogo, A.O.; Arce, A. Synchronization of cell division in *Euglena gracilis* by heat shock. *Exp. Cell Res.* **1964**, *36*, 390–397. [[CrossRef](#)]
54. Sinha, A.K.; Jaggi, M.; Raghuram, B.; Tuteja, N. Mitogen-Activated protein kinase signaling in plants under abiotic stress. *Plant Signal Behav.* **2011**, *6*, 196–203. [[CrossRef](#)] [[PubMed](#)]
55. Agrawal, G.K.; Rakwal, R.; Iwahashi, H. Isolation of novel rice (*Oryza sativa* L.) multiple stress responsive MAP kinase gene, *OsMSRMK2*, whose mRNA accumulates rapidly in response to environmental cues. *Biochem. Biophys. Res. Commun.* **2002**, *294*, 1009–1016. [[CrossRef](#)]
56. Li, C.; Kong, F.; Sun, P.P.; Bi, G.Q.; Li, N.; Mao, Y.X.; Sun, M.J. Genome-Wide identification and expression pattern analysis under abiotic stress of mitogen-activated protein kinase genes in *Pyropia yezoensis*. *J. Appl. Phycol.* **2018**, *30*, 2561–2572. [[CrossRef](#)]
57. Parages, M.L.; Figueroa, F.L.; Conde-Álvarez, R.M.; Jiménez, C. Phosphorylation of MAPK-like proteins in three intertidal macroalgae under stress conditions. *Aquat. Biol.* **2014**, *22*, 213–226. [[CrossRef](#)]
58. Zhao, F.Y.; Hu, F.; Zhang, S.Y.; Wang, K.; Zhang, C.R.; Liu, T. MAPKs regulate root growth by influencing auxin signaling and cell cycle-related gene expression in cadmium-stressed rice. *Environ. Sci. Pollut. Res.* **2013**, *20*, 5449–5460. [[CrossRef](#)]